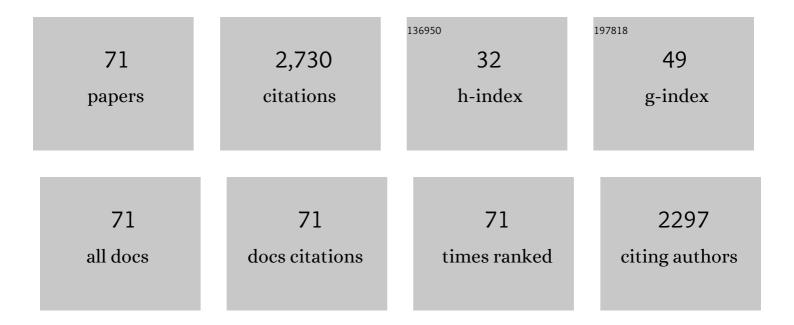
List of Publications by Year in descending order

Source: https://exaly.com/author-pdf/5055380/publications.pdf Version: 2024-02-01



#	Article	IF	CITATIONS
1	Improvement of Gas and Humidity Sensing Properties of Organ-like MXene by Alkaline Treatment. ACS Sensors, 2019, 4, 1261-1269.	7.8	232
2	The room temperature gas sensor based on Polyaniline@flower-like WO3 nanocomposites and flexible PET substrate for NH3 detection. Sensors and Actuators B: Chemical, 2018, 259, 505-513.	7.8	159
3	High-activity Mo, S co-doped carbon quantum dot nanozyme-based cascade colorimetric biosensor for sensitive detection of cholesterol. Journal of Materials Chemistry B, 2019, 7, 7042-7051.	5.8	98
4	Mixed-potential type NH3 sensor based on stabilized zirconia and Ni3V2O8 sensing electrode. Sensors and Actuators B: Chemical, 2015, 210, 795-802.	7.8	96
5	Ultrasensitive gas sensor based on hollow tungsten trioxide-nickel oxide (WO3-NiO) nanoflowers for fast and selective xylene detection. Journal of Colloid and Interface Science, 2019, 535, 458-468.	9.4	90
6	Integrating Target-Responsive Hydrogels with Smartphone for On-Site ppb-Level Quantitation of Organophosphate Pesticides. ACS Applied Materials & amp; Interfaces, 2019, 11, 27605-27614.	8.0	77
7	Realizing the Control of Electronic Energy Level Structure and Gas-Sensing Selectivity over Heteroatom-Doped In <sub>2</sub> O <sub>3</sub> Spheres with an Inverse Opal Microstructure. ACS Applied Materials & Interfaces, 2019, 11, 9600-9611.	8.0	76
8	Hydrothermal synthesis of hierarchical CoO/SnO2 nanostructures for ethanol gas sensor. Journal of Colloid and Interface Science, 2018, 513, 760-766.	9.4	75
9	The facile synthesis of MoO <sub>3</sub> microsheets and their excellent gas-sensing performance toward triethylamine: high selectivity, excellent stability and superior repeatability. New Journal of Chemistry, 2018, 42, 15111-15120.	2.8	73
10	Tandem catalysis driven by enzymes directed hybrid nanoflowers for on-site ultrasensitive detection of organophosphorus pesticide. Biosensors and Bioelectronics, 2019, 141, 111473.	10.1	72
11	MOF-Derived Mesoporous and Hierarchical Hollow-Structured In <sub>2</sub> O <sub>3</sub> -NiO Composites for Enhanced Triethylamine Sensing. ACS Sensors, 2021, 6, 3451-3461.	7.8	72
12	Self-Assembly Template Driven 3D Inverse Opal Microspheres Functionalized with Catalyst Nanoparticles Enabling a Highly Efficient Chemical Sensing Platform. ACS Applied Materials & Interfaces, 2018, 10, 5835-5844.	8.0	67
13	Mixed potential type acetone sensor using stabilized zirconia and M3V2O8 (M: Zn, Co and Ni) sensing electrode. Sensors and Actuators B: Chemical, 2015, 221, 673-680.	7.8	62
14	Smartphone-Assisted Robust Sensing Platform for On-Site Quantitation of 2,4-Dichlorophenoxyacetic Acid Using Red Emissive Carbon Dots. Analytical Chemistry, 2020, 92, 12716-12724.	6.5	58
15	Protein–Inorganic Hybrid Nanoflower-Rooted Agarose Hydrogel Platform for Point-of-Care Detection of Acetylcholine. ACS Applied Materials & Interfaces, 2019, 11, 11857-11864.	8.0	53
16	High-temperature NO2 gas sensor based on stabilized zirconia and CoTa2O6 sensing electrode. Sensors and Actuators B: Chemical, 2017, 240, 148-157.	7.8	52
17	Au <sub>39</sub> Rh <sub>61</sub> Alloy Nanocrystal-Decorated W <sub>18</sub> O <sub>49</sub> for Enhanced Detection of <i>n</i> Butanol. ACS Sensors, 2019, 4, 2662-2670.	7.8	47
18	Highly sensitive detection of Pb2+ and Cu2+ based on ZIF-67/MWCNT/Nafion-modified glassy carbon electrode. Analytica Chimica Acta, 2020, 1124, 166-175.	5.4	46

#	Article	IF	CITATIONS
19	Mesoporous ZnFe2O4 prepared through hard template and its acetone sensing properties. Materials Letters, 2016, 183, 378-381.	2.6	44
20	Fabrication of Well-Ordered Three-Phase Boundary with Nanostructure Pore Array for Mixed Potential-Type Zirconia-Based NO <sub>2</sub> Sensor. ACS Applied Materials & Interfaces, 2016, 8, 16752-16760.	8.0	41
21	High performance mixed-potential type NO2 sensors based on three-dimensional TPB and Co3V2O8 sensing electrode. Sensors and Actuators B: Chemical, 2015, 216, 121-127.	7.8	40
22	YSZ-based NO2 sensor utilizing hierarchical In2O3 electrode. Sensors and Actuators B: Chemical, 2016, 222, 698-706.	7.8	40
23	Novel Self-Assembly Route Assisted Ultra-Fast Trace Volatile Organic Compounds Gas Sensing Based on Three-Dimensional Opal Microspheres Composites for Diabetes Diagnosis. ACS Applied Materials & Interfaces, 2018, 10, 32913-32921.	8.0	40
24	A Redâ€Emissive Fluorescent Probe with a Compact Singleâ€Benzeneâ€Based Skeleton for Cell Imaging of Lipid Droplets. Advanced Optical Materials, 2020, 8, 1902123.	7.3	40
25	Gas sensor based on cobalt-doped 3D inverse opal SnO2 for air quality monitoring. Sensors and Actuators B: Chemical, 2022, 350, 130807.	7.8	40
26	Background-free sensing platform for on-site detection of carbamate pesticide through upconversion nanoparticles-based hydrogel suit. Biosensors and Bioelectronics, 2021, 194, 113598.	10.1	40
27	Fabrication of well-ordered porous array mounted with gold nanoparticles and enhanced sensing properties for mixed potential-type zirconia-based NH3 sensor. Sensors and Actuators B: Chemical, 2017, 243, 1083-1091.	7.8	37
28	A rapid-response room-temperature planar type gas sensor based on DPA-Ph-DBPzDCN for the sensitive detection of NH <sub>3</sub> . Journal of Materials Chemistry A, 2019, 7, 4744-4750.	10.3	37
29	Gas sensor based on samarium oxide loaded mulberry-shaped tin oxide for highly selective and sub ppm-level acetone detection. Journal of Colloid and Interface Science, 2018, 531, 74-82.	9.4	35
30	Fluorescent hydrogel test kit coordination with smartphone: Robust performance for on-site dimethoate analysis. Biosensors and Bioelectronics, 2019, 145, 111706.	10.1	35
31	All-Nanofiber Network Structure for Ultrasensitive Piezoresistive Pressure Sensors. ACS Applied Materials & Interfaces, 2022, 14, 19949-19957.	8.0	35
32	High-response and low-temperature nitrogen dioxide gas sensor based on gold-loaded mesoporous indium trioxide. Journal of Colloid and Interface Science, 2018, 524, 368-378.	9.4	34
33	Preparation of silver-loaded titanium dioxide hedgehog-like architecture composed of hundreds of nanorods and its fast response to xylene. Journal of Colloid and Interface Science, 2019, 536, 215-223.	9.4	33
34	Self-Assembly 3D Porous Crumpled MXene Spheres as Efficient Gas and Pressure Sensing Material for Transient All-MXene Sensors. Nano-Micro Letters, 2022, 14, 56.	27.0	33
35	YSZ-based mixed potential H2S sensor using La2NiO4 sensing electrode. Sensors and Actuators B: Chemical, 2018, 255, 3033-3039.	7.8	32
36	NASICON-based gas sensor utilizing MMnO3 (M: Gd, Sm, La) sensing electrode for triethylamine detection. Sensors and Actuators B: Chemical, 2019, 295, 56-64.	7.8	32

#	Article	IF	CITATIONS
37	Ethanol sensor using gadolinia-doped ceria solid electrolyte and double perovskite structure sensing material. Sensors and Actuators B: Chemical, 2021, 349, 130771.	7.8	27
38	Facile synthesis of nitrogen and sulfur co-doped carbon dots for multiple sensing capacities: alkaline fluorescence enhancement effect, temperature sensing, and selective detection of Fe <sup>3+</sup> ions. New Journal of Chemistry, 2018, 42, 13147-13156.	2.8	26
39	Lab in hydrogel portable kit: On-site monitoring of oxalate. Biosensors and Bioelectronics, 2020, 167, 112457.	10.1	26
40	Highly sensitive and selective xylene sensor based on p-p heterojunctions composites derived from off-stoichiometric cobalt tungstate. Sensors and Actuators B: Chemical, 2022, 351, 130973.	7.8	26
41	A TPA-DCPP organic semiconductor film-based room temperature NH3 sensor for insight into the sensing properties. Sensors and Actuators B: Chemical, 2021, 327, 128940.	7.8	25
42	Mixed potential type acetone sensor based on GDC used for breath analysis. Sensors and Actuators B: Chemical, 2021, 326, 128846.	7.8	24
43	Microwave gas sensor for detection of ammonia at room-temperature. Sensors and Actuators B: Chemical, 2022, 350, 130854.	7.8	24
44	Mixed potential type H2S sensor based on stabilized zirconia and a Co2SnO4 sensing electrode for halitosis monitoring. Sensors and Actuators B: Chemical, 2020, 321, 128587.	7.8	23
45	Gold-Trisoctahedra-Coated Capillary-Based SERS Platform for Microsampling and Sensitive Detection of Trace Fentanyl. Analytical Chemistry, 2022, 94, 4850-4858.	6.5	23
46	Stimulated Emission Depletion (STED) Super-Resolution Imaging with an Advanced Organic Fluorescent Probe: Visualizing the Cellular Lipid Droplets at the Unprecedented Nanoscale Resolution. , 2021, 3, 516-524.		22
47	Synthesis, characterization and gas sensing properties of porous flower-like indium oxide nanostructures. RSC Advances, 2015, 5, 30297-30302.	3.6	21
48	Acetone sensing with a mixed potential sensor based on Ce0.8Gd0.2O1.95 solid electrolyte and Sr2MMoO6 (M: Fe, Mg, Ni) sensing electrode. Sensors and Actuators B: Chemical, 2019, 284, 751-758.	7.8	21
49	Ultra-fast and low detection limit of H2S sensor based on hydrothermal synthesized Cu7S4-CuO microflowers. Sensors and Actuators B: Chemical, 2022, 350, 130847.	7.8	21
50	The Introduction of Defects in Ti <sub>3</sub> C <sub>2</sub> T <i><sub>x</sub></i> and Ti <sub>3</sub> C <sub>2</sub> T <i><sub>x</sub></i> â€Assisted Reduction of Graphene Oxide for Highly Selective Detection of ppbâ€Level NO <sub>2</sub> . Advanced Functional Materials, 2022, 32, .	14.9	21
51	Bioinspired laccase-mimicking catalyst for on-site monitoring of thiram in paper-based colorimetric platform. Biosensors and Bioelectronics, 2022, 207, 114199.	10.1	18
52	Insight into the effect of the continuous testing and aging on the SO2 sensing characteristics of a YSZ (Yttria-stabilized Zirconia)-based sensor utilizing ZnGa2O4 and Pt electrodes. Journal of Hazardous Materials, 2020, 388, 121772.	12.4	17
53	Machine Learning-Assisted Development of Sensitive Electrode Materials for Mixed Potential-Type NO <sub>2</sub> Gas Sensors. ACS Applied Materials & Interfaces, 2021, 13, 50121-50131.	8.0	16
54	Room-Temperature Mixed-Potential Type ppb-Level NO Sensors Based on K <sub>2</sub> Fe <sub>4</sub> O <sub>7</sub> Electrolyte and Ni/Fe–MOF Sensing Electrodes. ACS Sensors, 2021, 6, 4435-4442.	7.8	16

			CITATIONS
<sup>55</sup> The enhanced CO gas sensing performance of Pd/SnO <sub>2</sub> hollow sphere ser hydrothermal conditions. RSC Advances, 2016, 6, 80455-80461.	nsors under	3.6	15
56 Enhanced resistive acetone sensing by using hollow spherical composites prepared from In2O3. Mikrochimica Acta, 2019, 186, 359.	m MoO3 and	5.0	15
57 Specificity improvement of the YSZ-based mixed potential gas sensor for acetone and h detection. Sensors and Actuators B: Chemical, 2021, 341, 129292.	hydrogen sulfide	7.8	15
<ul> <li>Ti<sub>3</sub>C<sub>2</sub> MXene Nanosheets Functionalized with</li> <li>NaErF<sub>4</sub>:0.5%Tm@NaLuF<sub>4</sub> Nanoparticles for Dual-Modal Near</li> <li>Ilb/Magnetic Resonance Imaging-Guided Tumor Hyperthermia. ACS Applied Nano Mater</li> <li>8142-8153.</li> </ul>		5.0	15
59 Mixed potential type YSZ-based NO2 sensors with efficient three-dimensional three-pha processed by electrospinning. Sensors and Actuators B: Chemical, 2022, 354, 131219.		7.8	14
Improvement of NO <sub>2</sub> sensing characteristic for mixed potential type gas s 60 YSZ and Rh/Co <sub>3</sub> V <sub>2</sub> O <sub>8</sub> sensing electrode. RSC A 49440-49445.		3.6	11
Highly Selective Mixed Potential Methanol Gas Sensor Based on a 61 Ce <sub>0.8</sub> Gd <sub>0.2</sub> O <sub>1.95</sub> Solid Electrolyte and Au Sensors, 2022, 7, 972-984.	sing Electrode. ACS	7.8	9
62 Introduction of MWCNT for enhancing sensitivity of room-temperature mixed-potentia sensor attached with Ni-MOF sensing electrode. Sensors and Actuators B: Chemical, 20		7.8	9
63 Molecular Conformation Engineering To Achieve Longer and Brighter Deep Red/Near-In in Crystalline State. Journal of Physical Chemistry Letters, 2022, 13, 4754-4761.	frared Emission	4.6	9
<sup>64</sup> Novel quaternary oxide semiconductor for the application of gas sensors with long-terr Journal of Colloid and Interface Science, 2021, 592, 186-194.	m stability.	9.4	8
<sup>65</sup> Revealing the correlation between gas selectivity and semiconductor energy band structure from off-stoichiometric spinel CdGa2O4. Sensors and Actuators B: Chemical, 2022, 353	cture derived 2, 131039.	7.8	8
66 Understanding the Increasing Trend of Sensor Signal with Decreasing Oxygen Partial Pr Sensing-Reaction Model Based on O <sup>2–</sup> Species. ACS Sensors, 2022, 7, 2	ressure by a 1095-1104.	7.8	7
<sup>67</sup> Temperature-controlled resistive sensing of gaseous H2S or NO2 by using flower-like particular SnO2 nanomaterials. Mikrochimica Acta, 2020, 187, 297.	alladium-doped	5.0	6
<sup>68</sup> Self-assembled multiprotein nanostructures with enhanced stability and signal amplific capability for sensitive fluorogenic immunoassays. Biosensors and Bioelectronics, 2022	ration 2, 206, 114132.	10.1	6
69 Embedding Proteins within Spatially Controlled Hierarchical Nanoarchitectures for Ultra Immunoassay. Analytical Chemistry, 2022, 94, 6271-6280.	asensitive	6.5	6
70 Highly sensitive mixed-potential type ethanol sensors based on stabilized zirconia and 2 electrode. RSC Advances, 2016, 6, 27197-27204.	ZnNb2O6sensing	3.6	5
The Introduction of Defects in Ti <sub>3</sub> C <sub>2</sub> T <i><sub>x</sub></i> a Ti <sub>3</sub> C <sub>2</sub> T <i><sub>x</sub></i> a Selective Detection of ppbâ€Level NO <sub>2</sub> (Adv. Funct. Mater. 15/2022). Adv Materials. 2022. 32	ne Oxide for Highly	14.9	2